ORIGINAL RESEARCH

*Irp*2 Knockout Causes Osteoporosis by Inhibition of Bone Remodeling

Yaru Zhou[1] · Yu Yang[1] · Yan Liu[1] · Hengrui Chang[2] · Kuanzhi Liu[1] · Xiaojuan Zhang[1] · Yanzhong Chang[3]

Abstract
It has been found that iron disorder may lead to osteoporosis. However, the mechanism has been little explored. In the present study, we try to investigate the effects of iron disorder on bone metabolism using *Irp*2 knockout ($Irp2^{-/-}$) mice. Female $Irp2^{-/-}$ mice were used in this study. Bone mineral density (BMD) was measured by Micro-CT. Serum markers for bone turnover were measured by enzyme-linked immunosorbent assay. Content of iron was measured in bone and liver tissue, and Vitamin D 25-hydroxylase (CYP2R1) content was measured in liver tissue. Relative gene expression involved in iron export and uptake, and some genes involved in activities of osteoblast and osteoclast were all measured by real-time PCR and western blot. Compared to wild-type mice, $Irp2^{-/-}$ mice exhibited reduced BMD, bone iron deficiency, and hepatic iron overload. Serum levels of $25(OH)D_3$ and markers for bone formation such as bone alkaline phosphatase (Balp), bone-gla-protein (BGP), and type I collagen alpha1 chain (Col I α_1) were decreased, while markers for bone resorption including cathepsin K (Ctsk) and tartrate-resistant acid phosphatase (Trap) were all significantly increased. Hepatic CYP2R1 level was decreased in $Irp2^{-/-}$ mice compared with wild-type control mice. Compared to wild-type C57BL6 control mice, the expression of genes involved in osteoblast activity such as Balp, BGP, and Col I α_1 were all significantly decreased in bone tissue, while genes for osteoclast activity such as Ctsk and Trap were all markedly increased in $Irp2^{-/-}$ mice at mRNA level. Genes involved in iron storage, uptake, and exporting were also measured in bone tissue. Posttranscriptionally decreased ferritin (FTL), ferroportin 1 (FPN1), and increased transferrin receptor 1 (TfR1) gene expressions have been unexpectedly found in bone tissue of $Irp2^{-/-}$ mice. $Irp2^{-/-}$ mice exhibit reduced bone iron content and osteoporosis. Decreased circulating $25(OH)D_3$ levels promoted activity of osteoclast, while impaired activity of osteoblast may contribute to pathogenesis of osteoporosis. And, reduced bone iron content may not be totally caused by TfR1-dependent pathways.

Keywords Osteoporosis · Iron disorder · Hepatic · Bone tissue

Yaru Zhou and Yu Yang contributed equally to this work.

Electronic supplementary material The online version of this article (https://doi.org/10.1007/s00223-018-0469-2) contains supplementary material, which is available to authorized users.

✉ Yaru Zhou
zhouyaru_hc@163.com

✉ Yanzhong Chang
chang7676@163.com

1 Department of Endocrinology, Third Hospital of Hebei Medical University, Shijiazhuang, China

2 Department of Orthopaedic Surgery, Third Hospital of Hebei Medical University, Shijiazhuang, China

3 College of Life Science, Hebei Normal University, Shijiazhuang 050051, China

Introduction

Osteoporosis is one of the major public health problems; the prevalence and the severe consequences (i.e., fragility fractures) are increasing world-widely in paralleled with global population aging. The pathogenesis of osteoporosis is multifactorial and the environmental, iatrogenic, acquired, and genetic factors all have been suggested to be involved [1–3].

The correlation between iron disorders and osteoporosis has been recognized since 1997, which indicated that iron overload might be an independent risk factor for osteoporosis in patients with genetic hemochromatosis [4]. More studies have indicated that iron overload may cause bone weakening, including osteopenia and osteoporosis. In addition, it has been found that bone iron deficiency may also cause bone metabolic abnormalities, leading to decreased bone mineral density and bone strength, destructed bone

structure, and aggravating osteoporosis [5, 6]. However, the mechanisms underlying have been little explored. Bone remodeling is an important physiological process to preserve the structural integrity of the skeleton and is achieved through the balance between bone formation by osteoblasts and bone resorption by osteoclasts. Evidences accumulated in recent years have suggested that iron excess may disturb the homeostasis of bone remodeling [7, 8]. Iron overload may be correlated with osteoporosis in menopausal women [7]. In vitro studies have found that iron overload might inhibit osteoblast proliferation and differentiation [8], and inhibit osteoblast function through higher oxidative stress [9].

Vertebrate cellular iron metabolism is regulated posttranscriptionally by iron regulatory protein 1 (*Irp1*, also known as *Aco*1) and *Irp2* [10–12]. *Irps* are cytosolic RNA-binding proteins that bind to iron-responsive elements (*Ires*) located in the 59 or 39 untranslated regions of mRNAs encoding proteins of ferritin and transferring receptor (TfR), which are involved in iron sequestration and iron uptake, respectively. When cells become iron-depleted, *Irps* bind to *Ires* present in the mRNAs of ferritin and TfR1 with high affinity, resulting in diminished translation of the ferritin mRNA and increased translation of the transferring receptor mRNA. When cells are iron-sufficient, *Irp1* is converted to an [4Fe-4S]-containing aconitase while *Irp2* is degraded [13–15], leading to increased ferritin translation and promoted TfR1 mRNA degradation. It has been found that TfR1 may promote osteoclast differentiation and bone-resorbing activity, and promote mitochondrial respiration and production of reactive oxygen species [16]. Increased iron and transferrin levels can suppress alkaline phosphatase activity in osteoblasts due to higher oxidative stress [17].

It has been found that *Irp2* knockout (*Irp2$^{-/-}$*) mice exhibited osteoporosis with disturbed tissue iron distribution. In the present experiment, we will investigate some markers involved in bone formation, bone resorption, and iron metabolism in *Irp2$^{-/-}$* mice, to check the mechanisms underlying iron disorder in bone tissue and osteoporosis.

Materials and Methods

Animals

Irp2$^{-/-}$ mice (Purchased from MMRRC at UCDavis, USA, Cat. No. 030490-MU) and wild-type mice were the crossed generation of descendants of *Irp2$^{+/-}$* heterozygous mice. All animals were fed on standard rodent chow and tap water, and housed in a facility with temperature of 21 ± 2 °C and humidity of $55 \pm 10\%$ and under a 12-h dark/light cycle. Age-matched (15-month-old) C57BL/6 wild-type female mice and *Irp2$^{-/-}$* female mice were used in this study.

Genotype was determined by PCR amplification using the genomic DNA from tail clippings after treatment with proteinase K. The following primers were used for PCRs: Primer 1: 5′-AAA GAG TGG TCC ACT GTG AG-3′; Primer 2: 5′-TGG AAT ACC GGC AAT GGT GG-3′; Primer 3: 5′-AGC TCA TTC CTC CAC TCA TG-3′.

Bone Mineral Density (BMD) Measurement

BMD were measured by Micro-CT: The vertebrae (L5-6) were subjected to micro-computed tomography (Micro-CT) scans (SkyScan1176, Bruker). Three-dimensional images were reconstructed by an in-house volume-rendering software, which renders 3D views of the CT scan from arbitrary view points and directions, as well as measures the distance between two specific points. The lengths of vertebrae (L5–6) were measured on the reconstructed 3D images to provide BMD and trabecular number (Tb.N).

Histological Study on Bone Tissue

HE staining: The mice vertebral bones were excised, fixed in 4% paraformaldehyde (Sigma) for 48 h, decalcified with EDTA (Sigma) for 4 weeks, embedded in paraffin sectioned at 5 μm (Leica), and then subjected to staining with hematoxylin and eosin (Abcam, USA) according to the manual.

Prussian Blue Staining

Prussian blue staining was performed to determine the iron content in bone. Sections were deparaffinized and hydrated to distilled water. Equal volume of hydrochloric acid and potassium ferrocyanide was mixed immediately before use. Slices were immersed in this mixture solution for 30 min and then washed in distilled water. Counterstaining was performed with nuclear fast red and then slices were rinsed, dehydrated, and covered for observation. The number of blue granules in high-power field was recorded for calculation the iron content.

Measurement of Serum Iron, Calcium, and Biochemical Markers for Bone Turnover

Mice were anesthetized by intraperitoneal injection of 0.4% sodium pentobarbital. Blood was collected from retro-orbital sinus and centrifuged at $1000 \times g$ for 15 min at 4 °C, and serum was isolate and then stored at -80 °C until analysis. Serum iron and calcium concentrations were assessed by the Colorimetric method with kits (NanJing, JianCheng Bioengineering, China) according to the manufacturer's instructions.

Serum Balp, ColIα$_1$, BGP, Ctsk, Trap, and 25(OH)D$_3$ were measured by enzyme-linked immunosorbent assay (ELISA) (Shanghai Elisa Biotech Co., Ltd.).

Measurement of Iron, Calcium, and Phosphorus Content in Bone Tissue

Bone samples were digested in 65% spectra pure HNO3 (Merck) in the Microwave Digestion System (MARS 5, CEM Corp, USA) for 2 h at 100 μC, and then 4 h at 200 μC as described previously [18]. The totally digested samples were diluted to 2 ml with ultra-pure water. The concentrations of bone iron, calcium, and phosphorus were determined by atomic absorption spectrometry in conjunction with a graphite-furnace atomizer using an AA240FS apparatus (Varian, USA). The standard curves were plotted using serial concentrations of diluted standard solutions as described previously [19].

Determination of Hepatic Iron Levels and Vitamin D 25-Hydroxylase Content

Liver samples were digested in 65% spectra pure HNO3 (Merck) in the Microwave Digestion System (MARS 5, CEM Corp, USA) for 2 h at 100 μC, and then 4 h at 200 μC as described previously [18]. The totally digested samples were diluted to 2.5 ml with ultra-pure water. Hepatic content of vitamin D-25-hydroxylase (CYP2R1) in liver homogenates was performed by the method of ELISA kit with an automatic analyzer (SOFTmax PRO 4.3 LS).

Gene Expression Analysis by Quantitative Real-Time PCR (qRT-PCR)

The spine samples of mice were collected and dissected free of surrounding tissue, snap frozen in liquid nitrogen immediately, and then stored at −80 °C for RNA extraction. For RNA isolation, bone samples were homogenized in liquid nitrogen, and then transferred to TRIzol reagent (Invitrogen, San Diego, CA) according to the manufacturer's recommendation. Total RNA was purified using RNeasy kit (Qiagen, Valencia, CA.). RNA quality was checked by spectrophotometry and the ratio of A260/A280nm was calculated.

Genes involved in osteoporosis and iron metabolism were measured by real-time PCR. Total RNA (1 μg per sample) was reverse transcribed into cDNA using RT kit (Takara, Dalian, China). Gene expression was determined by monitoring SYBR green fluorescence intensity using an ABI 7900HT Fast Real-Time PCR System (Applied Biosystems, USA). Each PCR reaction (final volume: 20 μl) consisted of 5 ng cDNA, 10 μl of SYBR Green PCR master mix (Applied Biosystems Gen Star), and 150 nM of each PCR primer. PCR amplification was performed with the BIO-RAD CFX

Connect™ Optics Module with the following cycling parameters: 95 °C for 10 s, followed by 40 cycles at 95 °C for 15 s, and 60 °C for 1 min. Expression of GAPDH served as an internal control. Expression of the target gene was determined by normalizing to the respective GAPDH levels. The ΔΔCt method was used to compare fold changes in mRNA expression between wild-type control and $Irp2^{-/-}$ mice. Primer sequences were listed in *Supplementary material*.

Western Blot Analysis

Genes involved in iron metabolism were measured by western blot. Bone marrow cavity of mice was perfused with cold saline. Bones were isolated on ice and homogenized in lysis buffer (50 mM Tris, pH 7.5, 250 mM NaCl, 0.1 % sodium dodecyl sulfate (SDS), 2 mM dithiothreitol, 0.5 % NP-40, 1 mM phenylmethylsulfonyl fluoride (PMSF), and protease inhibitor cocktail on ice for 30 min). SDS-PAGE was performed as described previously [20]. Protein concentration was determined by Nanodrop-2000 (Thermo). Protein samples were subjected to SDS-polyacrylamide gel electrophoresis (SDS-PAGE) and transferred to nitrocellulose (NC) membranes. Membranes were incubated with mouse anti-rabbit Ferritin (1:1000) (Abcam, UK), mouse anti-rabbit FPN1 (1:5000) (Alpha Diagnostic International, USA), mouse anti-rat TfR1 (1:1000) (Invitrogen), and mouse anti-rabbit Actin (1:1000) (Abcam, UK) at 4 °C overnight, respectively, and then incubated with anti-rabbit (RPN4301, Amersham, UK) or anti-rat secondary antibody (RPN4201, Amersham, UK) conjugated to horseradish peroxide (1:10,000 dilution) for 90 min at room temperature. Blots were developed with ECL reagents (Pierce Biotechnology). Bands were quantified with densitometry software. Protein contents were normalized by Actin level (#T0004, affinity, USA).

Statistical Analysis

Statistical analysis was performed by SPSS software (version 21.0, SPSS Inc, Chicago). Normally distributed data were presented as means ± SD. Student's *t* tests were used for statistical analyses. *P* value less than 0.05 was considered statistically significant.

Results

Characterization of $Irp2^{-/-}$ Mice

In the present experiment, we found that both $Irp2^{-/-}$ mice and their control littermates developed osteoporosis (Fig. 1a–f). Compared to wild-type C57BL6 control mice, $Irp2^{-/-}$ mice exhibited markedly reduced trabecular

Fig. 1 $Irp2^{-/-}$ mice exhibited osteoporosis. Compared to $Irp2^{+/+}$ mice (**a, b**), $Irp2^{-/-}$ mice exhibited severe impaired trabecular architecture (**c–f**), markedly reduced BMD (**g**), and trabecular number (Tb.N) (**h**). (n = 6) *$P < 0.05$, **$P < 0.01$ vs. $Irp2^{+/+}$ mice, $Irp2^{+/+}$: white bar, $Irp2^{-/-}$: black bar
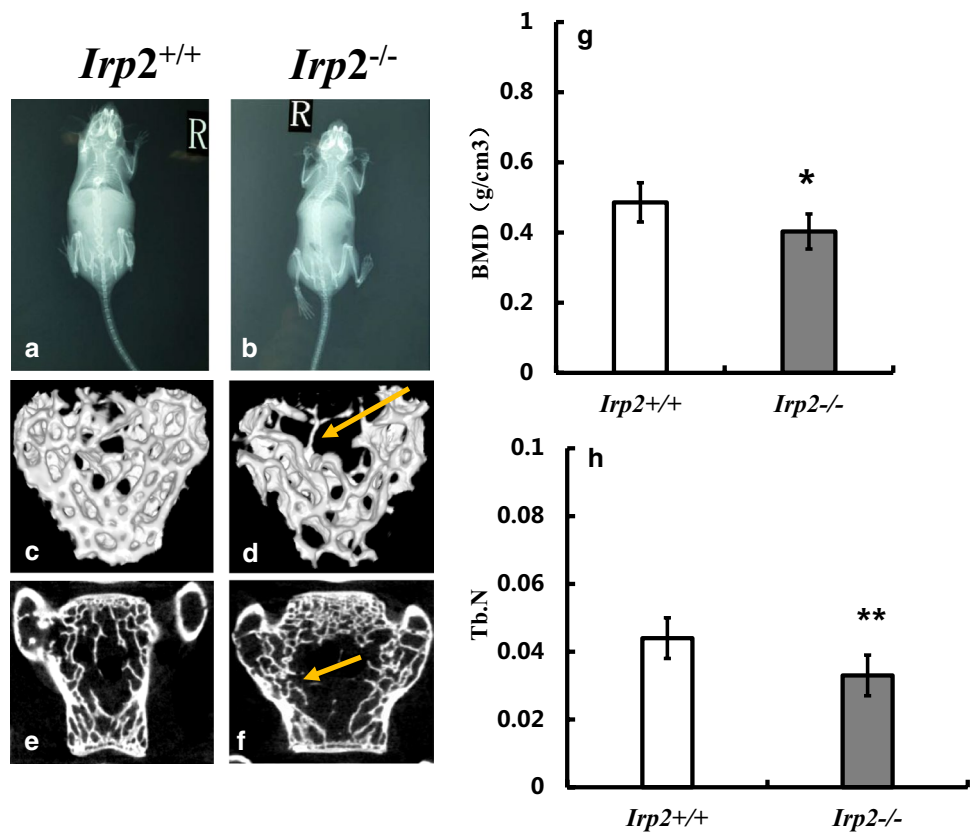
bone mass (both BMD and Tb.N) (Fig. 1g, h), and severe impaired trabecular architecture, indicating *Irp*2 knockout in mice led to impaired trabecular mass and trabecular architecture, contributing to severe osteoporosis.

Histological Results

HE staining showed that the trabecular bone was more sparse and thinner in $Irp2^{-/-}$ mice obvious decreased bone density and trabecular derangement could also be observed in $Irp2^{-/-}$ mice when compared with wild-type control (Fig. 2a, b).

Prussian blue staining indicted that blue granules were distributed sparsely inside the trabecular of wild-type C57BL6 control mice, demonstrating only few iron deposits in bone tissue. In contrast, iron blue particles were almost invisible in $Irp2^{-/-}$ mice (Fig. 2c, d). The numbers of blue granules were 12.33 ± 2.52 in wild-type control mice but 3.00 ± 1.00 in $Irp2^{-/-}$ mice, indicating reduced iron deposited in the bone tissue of $Irp2^{-/-}$ mice ($P < 0.01$) (Fig. 2e).

Parameters in Serum, Bone and Liver Tissue

The serum levels of $25(OH)D_3$ and iron were significantly lower in $Irp2^{-/-}$ mice when compared with wild-type control (Table 1). Compared to those in wild-type C57BL6 control mice, serum Balp, BGP, and Col I α_1 levels, which are the markers for bone formation, were significantly decreased (Table 1), while serum Ctsk and Trap, which are the markers for bone resorption, were pronounced higher in $Irp2^{-/-}$ mice (Table 1). There was no significant difference in serum calcium levels between the two groups (Table 1).

Compared to wild-type control mice, the levels of iron, calcium, and phosphorus in bone tissue were markedly decreased in $Irp2^{-/-}$ mice (Table 2). In addition, the concentration of hepatic CYP2R1 was also significantly reduced in $Irp2^{-/-}$ mice (Table 2). However, hepatic iron content was significantly increased in $Irp2^{-/-}$ mice, indicating iron overload in liver (Table 2).

Gene Expression

Compared to wild-type control mice, expressions of genes involved in osteoblast activity, Balp, BGP, and ColIα_1 were all significantly reduced at mRNA level in $Irp2^{-/-}$ mice (Fig. 3a–c). However, genes for osteoclast activity, such as Ctsk and Trap, were all markedly upregulated in $Irp2^{-/-}$ mice (Fig. 3d, e).

Genes involved in iron metabolism were measured in both mRNA and protein levels. Reduced expression of FPN1 were found in $Irp2^{-/-}$ mice at both mRNA and protein levels
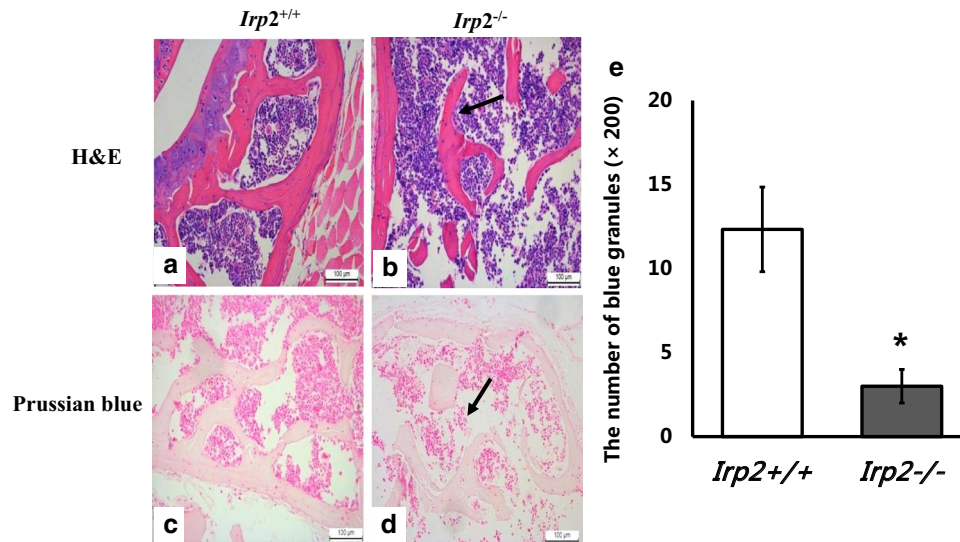
Fig. 2 Histological studies of the bone tissue from $Irp2^{-/-}$ and $Irp2^{+/+}$ mice. H&E staining showed that, compared to $Irp2^{+/+}$ mice, the trabecular bone was more sparse and thinner in $Irp2^{-/-}$ mice (**a, b**). Prussian blue staining indicted that blue granules was invisible in $Irp2^{-/-}$ mice when compared to $Irp2^{+/+}$ *mice* (**c, d**). The number of blue granules was significantly lower in the bone tissue of $Irp2^{-/-}$ mice than that of $Irp2^{+/+}$ mice, indicating reduced iron deposition in the bone tissue of $Irp2^{-/-}$ mice (**e**). (n = 3–4). Magnification: × 200, **$P < 0.01$ vs. $Irp2^{+/+}$ mice, $Irp2^{+/+}$: white bar, $Irp2^{-/-}$: black bar. (Color figure online)

Table 1 Parameters in serum

Group	$Irp2^{+/+}$ (n = 6)	$Irp2^{-/-}$ (n = 6)
Iron (µmol/l)	154.01 ± 65.096	64.71 ± 5.21**
Calcium (mmol/l)	1.62 ± 0.10	1.57 ± 0.12
25(OH)D3 (ng/ml)	28.40 ± 1.66	25.63 ± 0.98**
Balp (U/l)	166.66 ± 18.83	132.93 ± 4.82**
BGP (U/l)	2.86 ± 0.19	1.84 ± 0.17**
CoIIα$_1$ (ng/ml)	24.98 ± 2.04	20.21 ± 0.91**
Ctsk (U/l)	62.73 ± 7.00	72.42 ± 1.82*
Trap (U/l)	36.43 ± 2.77	40.63 ± 2.43*

*$P < 0.05$, **$P < 0.01$, $IRP2^{-/-}$ vs $IRP2^{+/+}$

Table 2 Parameters in bone and liver tissue

Group	$Irp2^{+/+}$ (n = 6)	$Irp2^{-/-}$ (n = 6)
Bone		
Iron (µg/g)	69.06 ± 11.21	45.54 ± 2.44**
Calcium (µg/g)	126460.61 ± 14905.81	98685.75 ± 10551.61*
Phosphorus (µg/g)	65188.45 ± 4104.76	52942.05 ± 5379.81**
Liver		
Iron (µg/g)	96.18 ± 49.30	221.03 ± 40.93**
Vitamin D 25-hydroxylase (ng/mg)	1.94 ± 0.13	1.21 ± 0.18**

*$P < 0.05$, **$P < 0.01$, $IRP2^{-/-}$ vs $IRP2^{+/+}$

when compared with controls, indicating reduced iron transportation from bone to plasma (Fig. 4a, d, e).

Ferritin contains 24 subunits of light (L) and heavy (H) chains. Ferritin-L (FTL) and Ferritin-H (FTH) are the main factors for cellular iron storage [21]. In this experiment, we found that although FTL was expressed higher in bone tissue in $Irp2^{-/-}$ mice at mRNA level, its expression was significantly reduced at protein level, which was combined with significantly reduced FTH expression, demonstrating that, as regards bone tissue FTL, there might be existing posttranscriptional modulations (Fig. 4b, d, f). Transferrin receptor 1 (TfR1), which corresponds to iron uptake, has been found with decreased expression in bone tissue in $Irp2^{-/-}$ mice at mRNA level; however, its expression was significantly increased at protein level (Fig. 4c, d, g).

Discussion

Iron plays an important role in physiological and biochemical processes. Recently, studies showed that abnormal iron metabolism, including iron deficiency or iron overload, is closely related to bone diseases [22, 23]. Bone iron deficiency may cause bone metabolic abnormalities, decrease bone mineral density, destruct bone structure, and reduce bone strength [5, 6], leading to aggravating osteoporosis, while iron overload also has been shown to cause similar consequences [22, 23].
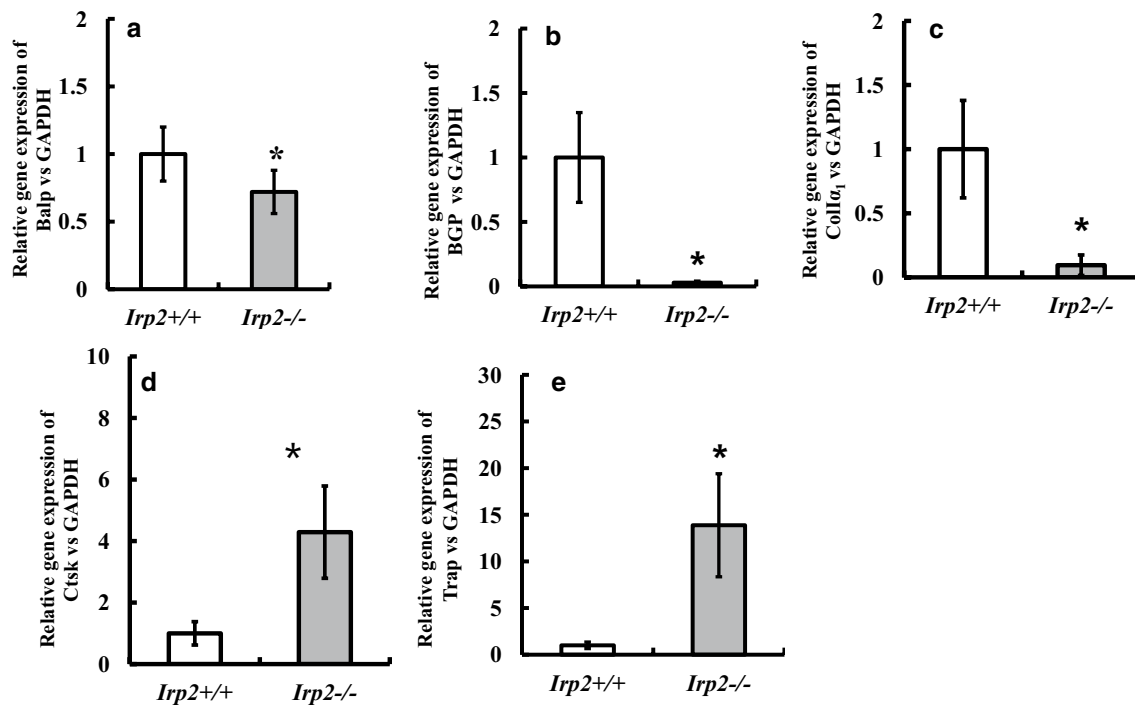
Fig. 3 Relative gene expression involved in bone metabolism. Compared to the wild-type control, expressions of genes involved in osteoblast activity such as *Balp, BGP*, and *Col Iα$_1$* were all significantly reduced at mRNA level in *Irp2$^{-/-}$* mice (**a–c**). However, genes involved in osteoclast activity, such as *Ctsk* and *Trap*, were all markedly upregulated in bone tissue of *Irp2$^{-/-}$* mice (**d, e**). ($n = 6$) *$P < 0.05$ **$P < 0.01$ vs. *Irp2$^{+/+}$* mice, *Irp2$^{+/+}$*: white bar, *Irp2$^{-/-}$*: black bar. Gene expressions were standardized to *GAPDH* mRNA
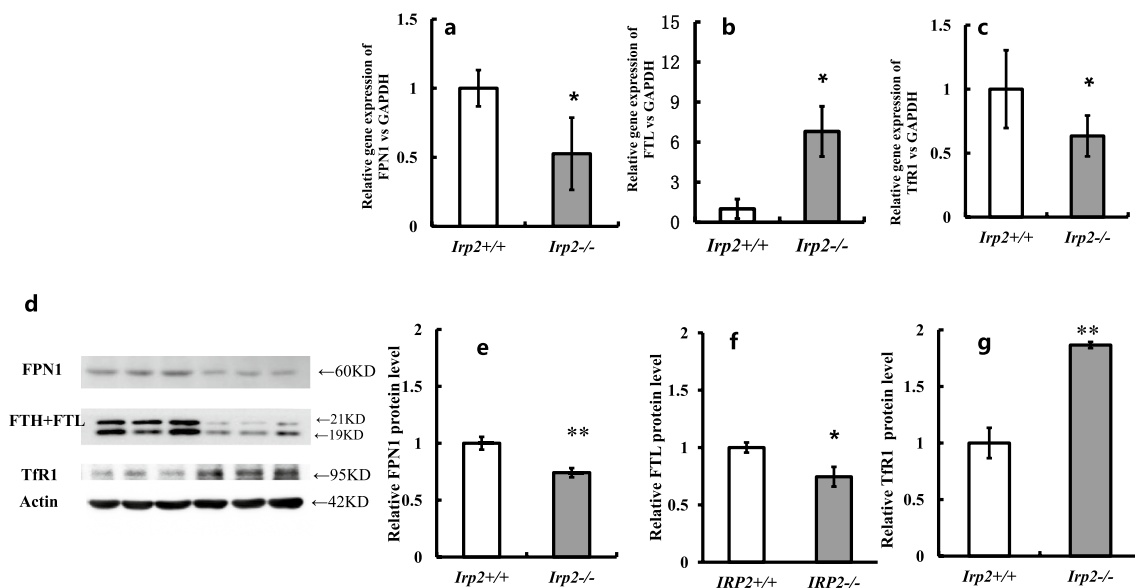

Fig. 4 Relative expressions of genes involved in iron metabolism were measured at both mRNA and protein levels. Compared with that of *Irp2$^{+/+}$* mice, Fpn1 expression was significantly lower in bone tissue of *Irp2$^{-/-}$* mice at both mRNA and protein levels (**a, d** and **e**). FTL was higher expressed in bone tissue in *Irp2$^{-/-}$* mice at mRNA level, but was significantly reduced at protein level (**b, d,** and **f**). The expression of TfR1 was decreased in bone tissue at mRNA level but significantly increased at protein level (**c, d,** and **g**) in *Irp2$^{-/-}$* mice. ($n = 6$) *$P < 0.05$ **$P < 0.01$ vs. *Irp2$^{+/+}$* mice, *Irp2$^{+/+}$*: white bar, *Irp2$^{-/-}$*: black bar. Protein expressions were standardized to Actin

Cellular iron homeostasis is maintained mainly by iron regulatory proteins 1 and 2 (*Irp1* and *Irp2*). Both *Irp1* and *Irp2*, especially the latter [24], may posttranscriptionally control the expression of several mRNAs encoding proteins involving iron metabolism, including ferritin (both H- and L-subunits) and TfR1, by binding to iron-responsive elements (IREs) in vivo [25] and in vitro [26]. Targeted disruption *Irp* may lead to distinct phenotypic abnormalities. $Irp1^{-/-}$ mice develop polycythemia and pulmonary hypertension, while $Irp2^{-/-}$ mice present with microcytic anemia, iron overload in brain, intestine, and liver, and neurologic defects [27, 28].

It has been found previously that iron overload in a variety of hematologic diseases is associated with excessive bone resorption [29]. However, the molecular mechanisms are not well understood. In the present experiment, we found that C57BL6 $Irp2^{-/-}$ mice exhibited osteoporosis. Bone remodeling is an important physiological process to preserve the structural integrity of the skeleton, and is achieved through the balance between bone formation and bone resorption. Vitamin D_3 is a steroid hormone that plays an important role in regulation of calcium and bone metabolism. In particular, Vitamin D stimulates bone formation. Vitamin D_3 can be activated after two sequential hydroxylation reactions: first in the liver to 25-(OH) D_3 and then in the kidney to 1,25-$(OH)_2$ vitamin D_3. Vitamin D 25-hydroxylase, also known as cytochrome P450 2R1 (CYP2R1), is an enzyme that is encoded by CYP2R1 gene in humans. It has been found previously that hepatic iron overload may correlate with osteoporosis [30, 31]. However, the mechanisms underlying have been poorly investigated. In the present experiment, we have found that $Irp2^{-/-}$ mice exhibited hepatic iron overload, reduced hepatic CYP2R1 content, and reduced circulating serum 25(OH)D_3 levels, which may contribute to reduced bone formation.

The balance between the activity of osteoblasts and osteoclasts is very important to maintain the hemostasis of bone remodeling [32], which can be measured by markers in circulation. Balp is a reliable marker for bone formation [33]. Bone γ-Carboxyglutamic acid-containing protein (BGP), also known as osteocalcin, is the most abundant non-collagenous bone matrix protein and accounts for 2% of bone mass [34]. Serum BGP level has been found to be a specific and sensitive marker for bone formation and bone mineralization [35, 36]. COLIα$_1$ is the major organic component in bone and it is expressed by mature osteoblasts [37]. Ctsk is highly and selectively expressed in osteoclasts [38], while Trap has been considered to be the marker of osteoclast differentiation. In the present study, we found that in $Irp2^{-/-}$ mice, serum levels of Balp, BGP, and COLIα were all significantly reduced, while levels of Ctsk and Trap were all increased.

Relative gene expression involved in bone turnover has also indicated that Balp, BGP, and COLIα$_1$ were significantly reduced while Ctsk and Trap were all increased at mRNA level in bone tissue, suggesting that deletion of *Irp*2 may impair bone formation while enhance bone absorption.

Histological studies showed overload iron deposition in the liver. Similar results have described by Galy et al., which indicated that young adult $Irp2^{-/-}$ mice displayed iron overload in the liver and duodenum, while iron deficient in the spleen [39]. And, in addition, we found damaged bone structure with less iron deposits in bone tissue in $Irp2^{-/-}$ mice.

Ferritin, the protein major for iron storage, which contains 24 subunits of light (L) and heavy (H) chains, plays a critical role in maintenance the intracellular iron balance [40]. Ferroportin (FPN), which is also termed as Slc40a1 or MTP1, is a unique factor for cellular iron exporting [41]. FPN1 is a major transmembrane iron export protein, corresponding for transporting iron from cell into the plasma [42–44]. TfR1-mediated iron uptake promotes osteoclast differentiation and bone-resorbing activity [16]. *Irp2* may sense cytosolic iron levels and posttranscriptionally regulate iron metabolism genes, including TfR1 and FTH and FTL. It has been found previously that $Irp2^{-/-}$ mice exhibit alerted iron distribution, the reasons of which are still under exploration. It has been found previously that $Irp2^{-/-}$ mice exhibited posttranscriptionally increased FTL and decreased TfR1 protein levels in brain, liver, kidney, and duodenum [25, 39, 45], which is consistent with iron accumulation in these tissues. However, it seemed that disturbed iron distribution in *Irp2* deficient mice could not be totally explained only by tissue ferritin, ferroportin, and TfR1 levels. Posttranscriptionally reduced ferritin and ferroportin expressions were noted in the spleen with reduced iron content in *Irp2*-deficient mice [39]. In the present experiment, we found that iron content was reduced in bone tissue. Due to the very limited data, so far the mechanisms are still unknown. We are first to check the gene expressions of FPN1, ferritin, and TfR1 in bone tissue. Data in the present experiment have shown that FPN1 gene expression was reduced at both mRNA and protein levels in $Irp2^{-/-}$ mice. FTL was higher at mRNA level but reduced at protein level, while TfR1, although found decreased at mRNA levels, was increased at protein level, indicating posttranscriptional regulations in FTL and TfR1 gene expression in bone tissue. In the present experiment, FPN1 and FTL all have been found decreased, while TfR1 was increased at protein level in bone tissue of $Irp2^{-/-}$ mice, which are similar to those found in spleen [39]. Since down regulated FTL and upregulated TfR1 should result in iron retention, reduced bone iron content found in $Irp2^{-/-}$ mice might be partly caused by TfR1-independent pathways. More detailed studies are still needed for further explanation of these findings.

Conclusions

*Irp*2 knockout may lead to iron redistribution and osteoporosis. Decreased hepatic $25(OH)D_3$ levels promoted activity of osteoclast, while impaired activity of osteoblast may contribute to pathogenesis of osteoporosis. Reduced iron content in bone tissue might not be totally caused by TfR1-dependent pathways.

Author Contributions YZ and YY performed most of the experiments; YL, HC, KL, and XZ performed experiments and data analysis; YY wrote the manuscript; YZ, YL, and YC interpreted data and critically revised the manuscript. All authors approved the final manuscript.

Compliance with Ethical Standards

Conflict of interest Yaru Zhou, Yu Yang, Yan Liu, Hengrui Chang, Kuanzhi Liu, Xiaojuan Zhang, and Yanzhong Chang declare that they have no conflict of interest.

Human and Animal Rights and Informed Consent The experimental procedures were carried out in accordance with the National Institutes of Health Guide for the Care and Use of Laboratory Animals, and were approved by the Animal Care and Use Committee of Hebei Science and Technical Bureau in China.

References

1. Rossi F, Perrotta S, Bellini G et al (2014) Iron overload causes osteoporosis in thalassemia major patients through interaction with transient receptor potential vanilloid type 1 (TRPV1) channels. Haematologica 99(12):1876–1884
2. Guggenbuhl P, Deugnier Y, Boisdet JF et al (2005) Bone mineral density in men with genetic hemochromatosis and HFE gene mutation. Osteoporos Int 16:1809–1814
3. Valenti L, Varenna M, Fracanzani AL (2009) et, al. Association between iron overload and osteoporosis in patients with hereditary hemochromatosis. Osteoporos Int 20:549–555
4. Sinigaglia L, Fargion S, Fracanzani AL et al (1997) Bone and joint involvement in genetic hemochromatosis: role of cirrhosis and iron overload. J Rheumatol 24(9):1809–1813
5. Medeiros DM, Plattner A, Jennings D et al (2002) Bone morphology, strength and density are compromised in iron-deficient rats and exacerbated by calcium restriction. J Nutr 132(10):3135–3141
6. Medeiros DM, Stoecker B, Plattener A et al (2004) Iron deficiency negatively affects vertebrae and femurs of rats independently of energy intake and body weight. J Nutr 134(11):3061–3067
7. Li GF, Pan YZ, Sirois P et al (2012) Iron homeostasis in osteoporosis and its clinical implications. Osteoporos Int 23:2403–2408
8. Yamasaki K, Hagiwara H (2009) Excess iron inhibits osteoblast metabolism. Toxicol Lett 191:211–215
9. He YF, Ma Y, Gao C et al (2013) Iron overload inhibits osteoblast biological activity through oxidative stress. Biol Trace Elem Res 152(2):292–296
10. Hentze MW, Muckenthaler MU, Galy B et al (2010) Two to tango:regulation of Mammalian iron metabolism. Cell 9(1):24–38 142(
11. Anderson CP, Shen M, Eisenstein RS et al (2012) Mammalian iron metabolism and its control by iron regulatory proteins. Biochim Biophys Acta 1823(9):1468–1483
12. Sanchez M, Galy B, Schwanhaeusser B et al (2011) Iron regulatory protein-1 and -2: transcriptome-wide definition of binding mRNAs and shaping of the cellular proteome by iron regulatory proteins. Blood 118(22):e168–e179
13. Vashisht AA, Zumbrennen KB, Huang X et al (2009) Control of iron homeostasis by an iron-regulated ubiquitin ligase. Science 326(5953):718–721
14. Salahudeen AA, Thompson JW, Ruiz JC et al (2009) An E3 ligase possessing an iron-responsive hemerythrin domain is a regulator of iron homeostasis. Science 326(5953):722–726
15. Moroishi T, Nishiyama M, Takeda Y et al (2011) The FBXL5-IRP2 axis is integral to control of iron metabolism in vivo. Cell Metab 14(3):339–351
16. Ishii KA, Fumoto T, Iwai K et al (2009) Coordination of PGC-1beta and iron uptake in mitochondrial biogenesis and osteoclast activation. Nat Med 15(3):259–266
17. Yang Q, Jian J, Abramson SB et al (2011) Inhibitory effects of iron on bone morphogenetic protein 2-induced osteoblastogenesis. J Bone Miner Res 26:1188–1196
18. Chang YZ, Qian ZM, Wang K et al (2005) Effects of development and iron status on ceruloplasmin expression in rat brain. J Cell Physiol 204(2):623–631
19. Machado I, Bergmann G, Pistón M (2016) A simple and fast ultrasound-assisted extraction procedure for Fe and Zn determination in milk-based infant formulas using flame atomic absorption spectrometry (FAAS). Food Chem 194:373–376
20. Shi ZH, Nie G, Duan XL, Rouault T, Wu WS, Ning B, Zhang N, Chang YZ, Zhao BL (2010) Neuroprotective mechanism of mitochondrial ferritin on 6-hydroxydopamine-induceddopaminergic cell damage: implication for neuroprotection in Parkinson's disease. Antioxid Redox Signal 2010;13(6):783–796
21. Winter WE, Bazydlo LA, Harris NS (2014) The molecular biology of human iron metabolism. Lab Med 45(2):92–102
22. Li J, Hou Y, Zhang S et al (2013) Excess iron undermined bone load-bearing capacity through tumor necrosis factor-alpha-dependent osteoclastic activation in mice. Biomed Rep 1:85–88
23. D'Amelio P, Cristofaro MA, Tamone C et al (2008) Role of iron metabolism and oxidative damage in postmenopausal bone loss. Bone 43:1010–1015
24. Meyron-Holtz EG, Ghosh MC, Rouault TA (2004) Mammalian tissue oxygen levels modulate iron-regulatory protein activities in vivo. Science 306:2087–2090
25. Meyron-Holtz EG, Ghosh MC, Iwai K et al (2004) Genetic ablations of iron regulatory proteins 1 and 2 reveal why iron regulatory protein 2 dominates iron homeostasis. EMBO J 23:386–395
26. Kim HY, Klausner RD, Rouault TA (1995) Translational repressor activity is equivalent and is quantitatively predicted by in vitro RNA binding for two iron-responsive element binding proteins, IRP1 and IRP2. J Biol Chem 270:4983–4986
27. Ghosh MC, Zhang DL, Jeong SY et al (2013) Deletion of iron regulatory protein 1 causes polycythemia and pulmonary hypertension in mice through translational derepression of HIF2α. Cell Metab 17(2):271–281
28. Cooperman SS, Meyron-Holtz EG, Olivierre-Wilson H et al (2005) Microcytic anemia, erythropoietic protoporphyria, and neurodegeneration in mice with targeted deletion of iron-regulatory protein 2. Blood 106(3):1084–1091
29. Zhou J, Ye S, Fujiwara T et al (2013) Steap4 plays a critical role in osteoclastogenesis in vitro by regulating cellular iron/reactive oxygen species (ROS) levels and cAMP response

element-binding protein (CREB) activation. J Biol Chem 288(42):30064–30074

30. Guggenbuhl P, Fergelot P, Doyard M et al (2011) Bone status in a mouse model of genetic hemochromatosis. Osteoporos Int 22(8):2313–2319

31. Doyard M, Chappard D, Leroyer P et al (2016) Decreased bone formation explains osteoporosis in a genetic mouse model of hemochromatosiss. PLoS ONE 11(2):e0148292

32. Mediero A, Cronstein BN (2013) Adenosine and bone metabolism. Trends Endocrinol Metab 24(6):290–300

33. Uemura H, Yasui T, Kiyokawa M et al (2002) Serum osteoprotegerin/osteoclastogenesis-inhibitory factor during pregnancy and lactation and the relationship with calcium-regulating hormones and bone turnover markers. J Endocrinol 174(2):353–359

34. Price PA, Parthemore JG, Deftos LJ (1980) New biochemical marker for bone metabolism. Measurement by radioimmunoassay of bone GLA protein in the plasma of normal subjects and patients with bonedisease. J Clin Invest 66(5):878–883

35. Zoch ML, Clemens TL, Riddle RC (2016) New insights into the biology of osteocalcin. Bone 82:42–49

36. Song YE, Tan H, Liu KJ et al (2011) Effect of fluoride exposure on bone metabolism indicators ALP, BALP, and BGP. Environ Health Prev Med 16(3):158–163

37. Kemper O, Herten M, Fischer J et al (2014) Prostacyclin suppresses twist expression in the presence of indomethacin in bone marrow-derived mesenchymal stromal cells. Med Sci Monit 20:2219–2227

38. Inui T, Ishibashi O, Inaoka T et al (1997) Cathepsin K antisense oligodeoxynucleotide inhibits osteoclastic bone resorption. J Biol Chem 272(13):8109–8112

39. Galy B, Ferring D, Minana B et al (2005) Altered body iron distribution and microcytosis in mice deficient in iron regulatory protein 2 (IRP2). Blood 106(7):2580–2589

40. Arosio P, Elia L, Poli M (2017) Ferritin, cellular iron storage and regulation. IUBMB Life 69(6):414–422

41. Ganz T (2005) Cellular iron: ferroportin is the only way out. Cell Metab 1(3):155–157

42. Rochette L, Gudjoncik A, Guenancia C et al (2015) The iron-regulatory hormone hepcidin: a possible therapeutic target? Pharmacol Ther 146:35–52

43. Wang G, Shao A, Hu W et al (2015) Changes of ferrous iron and its transporters after intracerebral hemorrhage in rats. Int J Clin Exp Pathol 8(9):10671–10679

44. Rice AE, Mendez MJ, Hokanson CA et al (2009) Investigation of the biophysical and cell biological properties of ferroportin, a multipass integral membrane protein iron exporter. J Mol Biol 386(3):717–732

45. Zumbrennen-Bullough KB, Becker L, Garrett L et al (2014) Abnormal brain iron metabolism in Irp2 deficient mice is associated with mild neurological and behavioral impairments. PLoS ONE 9(6):e98072